RADIOCARBON, Vol 48, Nr 3, 2006, p 355–372

HIGH-ACCURACY ^{14}C MEASUREMENTS FOR ATMOSPHERIC CO_2 SAMPLES BY AMS

H A J Meijer[1] • M H Pertuisot • J van der Plicht

Centrum voor IsotopenOnderzoek, University of Groningen, the Netherlands.

ABSTRACT. In this paper, we investigate how to achieve high-accuracy radiocarbon measurements by accelerator mass spectrometry (AMS) and present measurement series (performed on archived CO_2) of $^{14}CO_2$ between 1985 and 1991 for Point Barrow (Alaska) and the South Pole. We report in detail the measurement plan, the error sources, and the calibration scheme that enabled us to reach a combined uncertainty of better than ±3‰. The $\delta^{13}C$ correction and a suggestion for a span (or 2-point) calibration for the ^{14}C scale are discussed in detail. In addition, we report new, accurate values for the calibration and reference materials Ox2 and IAEA-C6 with respect to Ox1. The atmospheric $^{14}CO_2$ records (1985–1991) are presented as well and are compared with other existing records for that period. The Point Barrow record agrees very well with the existing Fruholmen (northern Norway) record from the same latitude. The South Pole record shows a small seasonal cycle but with an extreme phase with a maximum on January 1st (±13 days). Together with its generally elevated ^{14}C level compared to the Neumayer record (coastal Antarctica), this makes our South Pole data set a valuable additional source of information for global carbon cycle modeling using $^{14}CO_2$ as a constraint.

INTRODUCTION

In the 20th century, the radiocarbon concentration in atmospheric CO_2 was profoundly influenced by 2 human activities:

1. The massive above-ground bomb tests of the 1950s and 1960s have lead to a doubling of the pre-bomb ^{14}C concentration in the Northern Hemisphere (see e.g. Nydal and Lövseth 1983 and references therein). After the Test Ban Treaty in 1963, however, this ^{14}C excess decreased rapidly (to a good approximation exponentially, with a decay time of ~17 yr) by atmospheric CO_2 exchange with the oceans and the terrestrial biosphere. Thereby, both oceanic dissolved CO_2 and terrestrial carbon were to some extent enriched in ^{14}C.
2. The continuous and increasing combustion of fossil fuel delivers a load of ^{14}C-free CO_2 into the atmosphere, thereby diluting the atmospheric ^{14}C concentration. This process, called the Suess effect (Suess 1955), had been discovered in tree rings already in the 1950s.

The 2 effects combined lead to a continuous disequilibrium in the ^{14}C content of the different reservoirs of the carbon cycle: ocean, atmosphere, and terrestrial biosphere (both above-ground and in soils). Thanks to this disequilibrium, which was largest in the 1960s but still is measurable in the present day, careful and accurate long-term observation of atmospheric $^{14}CO_2$ forms an excellent tool for monitoring the carbon cycle, including fossil-fuel consumption (Levin et al. 1992, 2003; Levin and Hesshaimer 2000). The spatiotemporal pattern of atmosphere-ocean and atmosphere-biosphere interactions, as well as of fossil-fuel CO_2 sources, can be observed as $^{14}CO_2$ gradients in the atmosphere. However, due to the fast mixing characteristics of the atmosphere, the signals are small, and the best possible accuracy is needed.

High-accuracy ^{14}C measurements have, to date, only been produced using proportional gas counting. Provided a large quantity of material is available for both samples and standards (tens of liters of CO_2), and with an exceptional amount of time invested, combined uncertainties[2] below ±2‰ can

[1]Corresponding author. Email: h.a.j.meijer@rug.nl.

[2]"Combined uncertainty" (often called "accuracy") is the International Standards Organization [ISO] (1993) terminology for the combination of "Type A" (random effects) and "Type B" (systematic effects shared by 1 measurement series or 1 laboratory, such as the calibration uncertainty) uncertainty. Type A uncertainty is associated with "precision," whereas the combined uncertainty is associated with "accuracy."

https://doi.org/10.1017/S0033822200038807 Published online by Cambridge University Press

be achieved for samples <1 half-life old (Tans et al. 1979; de Jong 1981). However, this high accuracy can only be achieved on very special occasions for which the huge effort can be justified, such as dendrochronological absolute age calibration material (see Reimer et al. 2004 and references therein). Routine results for a proportional counter ^{14}C measurement of contemporary samples are typically ±5‰. This accuracy can be improved on relatively easily by extending the counting time, but for normal procedures and sample amounts, a combined uncertainty of ±2–3‰ seems to be the practical limit (van der Plicht and Bruins 2005).

For global studies of ^{14}C in atmospheric CO_2, combined uncertainties in this range are now generally reported (see e.g. Levin and Kromer 2004). To date, virtually all such measurement series have been measured using proportional counters, which typically require liters of CO_2 and, consequently, tens of m^3 of air. Most sample programs have used and are using an in situ CO_2 collection technique, usually by absorbing CO_2 from a flow of air in a NaOH bath. This makes sampling for $^{14}CO_2$ analysis a somewhat complicated matter that requires a special infrastructure.

Currently, there are many sites in the world where a sample of air is collected, usually twice a month, for analysis of various properties in the lab (trace gas concentrations, stable isotopes of CO_2, etc.). The amount of air collected ranges between 0.5 and 5 L. It would be practical and cost-effective if a $^{14}CO_2$ analysis could also be performed on these samples. Due to the amount of CO_2 present, however, this analysis would require the use of accelerator mass spectrometry (AMS), which poses a challenge to AMS to show that this technique can perform measurements with a combined uncertainty of ±3‰ or better.

The first reports are now appearing on AMS ^{14}C data of such air samples. Kitagawa et al. (2004) used air samples of ~8 L STP collected onboard container freight ships sailing the Pacific Ocean, whereas Turnbull et al. (2006) report first measurements on 2- to 4-L samples from continental sites in the USA. The present paper (of which first results have been published by van der Plicht et al. [2000]) describes our use of AMS for atmospheric $^{14}CO_2$ analysis of a 7-yr series of samples from the atmospheric sampling stations in the South Pole and Point Barrow (Alaska) from the Scripps Institute of Oceanography network (Keeling et al. 1989; Keeling and Whorf 2005). The samples from 1985–1991 were stored in Pyrex® flame-off tubes after stable isotope analysis (Roeloffzen et al. 1991). In this paper, we report in detail the measurement plan, the error sources, and the calibration scheme that enabled us to reach a combined uncertainty of ≤ ±3‰. The $^{14}CO_2$ results themselves are presented as well and are compared with other existing records for that period.

MEASUREMENTS

A total of 149 CO_2 gas samples were available for AMS ^{14}C analysis, equally distributed between the South Pole and Point Barrow, and evenly distributed over the years 1985–1991 (inclusive). Originally, this CO_2 had been extracted from sample flasks containing 5 L of air. Usually, the extracted CO_2 of several flasks (2 or 3, or occasionally even 4 or 5, from consecutive measurement weeks) had been put together in 1 flame-off tube.

The tubes were broken in the standard inlet arrangement of our dual-inlet stable isotope ratio mass spectrometer, and a stable isotope measurement was performed on the same SIRA-9 instrument used in the original analyses (Roeloffzen et al. 1991). We took care that contamination due to memory effects was kept to a minimum. The CO_2 was then frozen into a sample flask with an O-ring stopcock, removed from the isotope ratio mass spectrometer (IRMS), and connected to our graphitization system (Aerts-Bijma et al. 1997). For the majority of the samples (139), the amount of CO_2 was sufficient for our regular, 2-mm-diameter AMS targets, containing about 1.5 mg of C. For 45 of

these, even 2 targets could be produced from 1 CO_2 flask; these cases will be referred to as "full duplos." In 10 cases, however, the amount of CO_2 was only sufficient for a reduced-size target (ø 1 mm), and the graphitization was performed on our special low-volume system. These samples originated from only 1 original 5-L flask.

For all samples, the amount of CO_2 gas and C were measured volumetrically and gravimetrically, respectively. On average, the final amounts of C corresponded well to the amounts expected from aliquots of 5 L of air at atmospheric pressure, although the spread was considerable. Target pressing was done according to our standard procedures, using our automatic target press (Aerts-Bijma et al. 1997). The complete procedure resulted in 194 targets, 10 of which were reduced in size.

The samples were organized into 6 different batches, one of them dedicated to the small samples. Care was taken to randomize the position of the samples such that no spurious trends could be introduced (e.g. by drifts of the AMS) into the atmospheric records. Also, the full duplos were randomly distributed.

Typically, a batch consisted of 40 samples, including 8 samples of the Ox1 calibration standard, 4 samples of the IAEA C6 (ANU sucrose) reference material, and 4 backgrounds (Rommenhöller CO_2 gas). The addition of 4 C6 standards was expected to be fruitful for 2 reasons: 1) Ox1 and C6 function as a "scale span" since all samples to be measured have ^{14}C activities between these 2 extremes; and 2) to serve as independent batch calibration check.

The material for these standards had been combusted in 1 large-scale combustion, using the sample combustion system of our conventional ^{14}C laboratory. The CO_2 was kept in stainless steel cylinders. The individual standard samples were graphitized along with the atmospheric CO_2 samples for each specific batch to which they belonged, so that any (day-to-day) variability in the graphitization circumstances would be visible in the standards. The amount of CO_2 used was the same as for the samples. For the small samples, a smaller amount of CO_2 was used for the standards.

The batches were analyzed on the Groningen AMS, a 2.5MV Tandetron accelerator built by High Voltage Engineering Europa (van der Plicht et al. 2000). Each sample was analyzed following the standard procedure: 40-min analysis time consisting of 80 periods (blocks) of 30 s. Each block corresponds to a measurement on 1 sputter position of the Cs ion beam at the graphite surface. For each sample, we used 8 different sputter positions, for both the 2- and 1-mm diameter targets. During the total measurement time of 40 min, typically 160,000 ^{14}C counts were accumulated for Ox1 (and proportionally higher for IAEA-C6 and the samples).

After completion of a batch, a full remeasurement of the same batch was started, without removing the samples from the AMS ion source chamber. Only in the case of the 1-mm samples was reanalysis not possible due to the low amount of C. The results of this reanalysis will be referred to as "measurement duplos."

The total of 11 batches (5 of them being thus measurement duplos) were analyzed using our standard procedures. The Ox1 samples were used as a calibration standard for both ^{14}C and ^{13}C, i.e. the average value for the 8 samples in each batch was taken to represent the defined ^{14}C activity ratio $^{14}a^0_{Ox1N} = 1.0398$, corrected for isotope fractionation using $\delta^{13}C = -19‰$. The presence of 8 individual Ox1 samples enabled us, in principle, to observe any temporal drifts during the batch measurement. However, in none of the 11 batches was such a drift recognizable beyond the statistical errors. The 4 IAEA-C6 samples were treated as if they were "unknown" samples. The final results

https://doi.org/10.1017/S0033822200038807 Published online by Cambridge University Press

for all samples are reported as isotope- and sample yr-corrected delta values, denoted $^{14}\delta_N^S$ according to Mook and van der Plicht (1999), but more commonly as $\Delta^{14}C$ (Stuiver and Polach 1977).

DATA ANALYSIS

The complete set of measurements, including a total of 80 Ox1 and 40 C6 measurements, constitute a wealth of data. The high number of standards, the use of 2 different standards, the almost complete set of measurement duplos, and the 45 "full duplo" measurements allowed us to take a closer look at the performance of our AMS ^{14}C facility, as well as, of course, to produce the set of atmospheric measurements with the highest possible accuracy. More specifically, we investigated 2 aspects of the data that allowed for further improvement: $\delta^{13}C$ corrections and calibration and quality checks.

$\delta^{13}C$ Corrections

All ^{14}C activities are corrected for isotope fractionation using their $\delta^{13}C$ value relative to $\delta^{13}C = -25‰$ on the international VPDB scale (Mook and van der Plicht 1999). Apart from the more fundamental question of whether this fractionation correction is indeed fully applicable to atmospheric CO_2, one can also raise the question of whether or not all $\delta^{13}C$ variability one observes in the AMS measurements is caused by fractionation effects that indeed obey the mass-dependent fractionation rule:

$$\frac{^{14}a}{^{14}a_N} = \left(\frac{^{13}R}{^{13}R_N}\right)^{\theta} \quad (1)$$

in which ^{14}a and ^{13}R refer to the measured activity ratio and $^{13}C/^{12}C$ ratio, respectively; $^{14}a_N$ is the normalized ^{14}C activity; and $^{13}R_N$ is the $^{13}C/^{12}C$ ratio corresponding to $\delta^{13}C = -25‰$ (Mook and van der Plicht 1999). The exponent θ is by convention taken as 2.

Many of the fractionations that occur (such as those caused by incomplete graphitization and mass-dependent fractionation during the target sputtering process) can indeed successfully be corrected using Equation 1. However, it cannot be excluded that non-mass-dependent fractionation also occurs, or rather that the total AMS efficiency for ^{13}C varies in comparison to that of ^{14}C in a way not described by Equation 1. Finally, of course, random noise causes the $\delta^{13}C$ values to scatter without any relation to the ^{14}C measurements. The fact that we can compare the AMS $\delta^{13}C$ measurements to the original CO_2 gas IRMS measurements, as well as to their measurement duplo values, gives us a unique possibility to discriminate between these 2 $\delta^{13}C$ effects.

The fractionation caused by our graphitization systems has been investigated before (Aerts-Bijma et al. 1997). This investigation showed that our graphitization is in practice 100% efficient, and that residual fractionation effects are below 0.5‰. This implies that the majority of the difference between the IRMS and the AMS $\delta^{13}C$ measurement must be due to fractionations or drifts occurring in the AMS system.

Figure 1 presents the $\delta^{13}C$ values for one of the AMS batches. The figure shows both AMS $\delta^{13}C$ results (for the initial measurement and the measurement duplo) as well as the IRMS measurements. From this plot, as well as from the data of the other batches, it is clear that the AMS measurement process itself is the cause of the frequent ^{13}C deviations; the first and second measurement (measurement duplos) in the same batch, i.e. on the same graphite, show a considerable scatter, both with respect to each other and with respect to the IRMS measurement. The cases for which both AMS

https://doi.org/10.1017/S0033822200038807 Published online by Cambridge University Press

measurements deviate from the IRMS measurement but agree with each other are rare (and apparently coincidental).

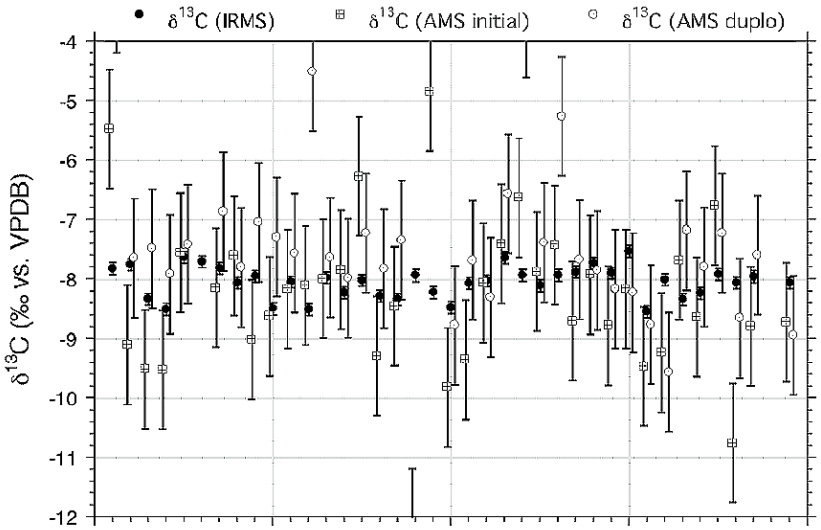

Figure 1 $\delta^{13}C$ values for one of the AMS batches. The figure shows both AMS $\delta^{13}C$ results (for the initial measurement and the measurement duplo on the same targets) as well as the IRMS measurement. The AMS measurement process itself (probably mainly the sputtering process) is the largest cause of ^{13}C scatter. If the $\delta^{13}C$ value for the AMS is outside the ±2‰ band around the "true" (IRMS) value, this almost always coincides with bad target quality (low current and thus low count rates), and these measurements usually had to be discarded.

Since this project yields so many detailed measurements, we decided to investigate the $\delta^{13}C_{AMS}$ - ^{14}a relation in detail. For the correction using the $\delta^{13}C_{AMS}$ of each individual sample, we applied, according to convention, Equation 1 with $\theta = 2$. To investigate if this choice was optimal, we compared the scatter in individual ^{14}a values with individual $\delta^{13}C$ values. This comparison, however, is only useful if we know the "true" $^{14}a_N$ value for the material under consideration. This restricted our study to the 2 calibration/reference materials Ox1 and C6 that we used. If we linearize Equation 1, using a Taylor expansion to first order, we arrive at:

$$\frac{^{14}a}{\overline{^{14}a_N}} = \frac{1}{(0.975)^{\theta}} + \frac{\theta}{(0.975)^{\theta}}\delta^{13}C_{AMS} \qquad (2)$$

in which the factor 0.975 = (1–25‰) is the standard $\delta^{13}C$ value; and $\overline{^{14}a_N}$ is the known $\delta^{13}C$-corrected activity for the material, which is 1.0398 for Ox1 and 1.5072 for C6 (see text below for this specific value).

Fitting Equation 2 to the data yielded values for θ closely equal to 2 within the error bars. These fits, however, are not "fair" tests for the value of θ, nor for the validity of corrections according to Equation 1, since the $\overline{^{14}a_N}$ values themselves have been deduced using Equation 1 with $\theta = 2$, and these values influence the fit in a major way through the intercept.

https://doi.org/10.1017/S0033822200038807 Published online by Cambridge University Press

A much better, independent way to test the ^{14}a-δ^{13}C relation is to use the relation between the difference in $\delta^{13}C_{AMS}$ values for the initial and duplo measurements ($\Delta\delta^{13}C_{AMS}$) and the difference in ^{14}a (Δ^{14}a). This removes the intercept for Equation 2:

$$\frac{\Delta^{14}a}{{}^{14}a_N} = \frac{\theta}{(0.975)^{\theta}}\Delta\delta^{13}C_{AMS} \tag{3}$$

A fit using Equation 3 will now independently verify the validity of the δ^{13}C-correction practice. Furthermore, the measured Ox1 and C6 can now be combined. The results are shown in Figure 2. We found θ to equal 1.92 ± 0.23. The correlation coefficient was 0.74, indicating that the standard deviation of the Δ^{14}a, and thus of the ^{14}a themselves as well, will be lowered by about one-third[3] by applying Equation 1; in other words, the standard deviation of $^{14}a_N$ will be lower than that of ^{14}a by about one-third, thanks to the fractionation correction using $\delta^{13}C_{AMS}$.

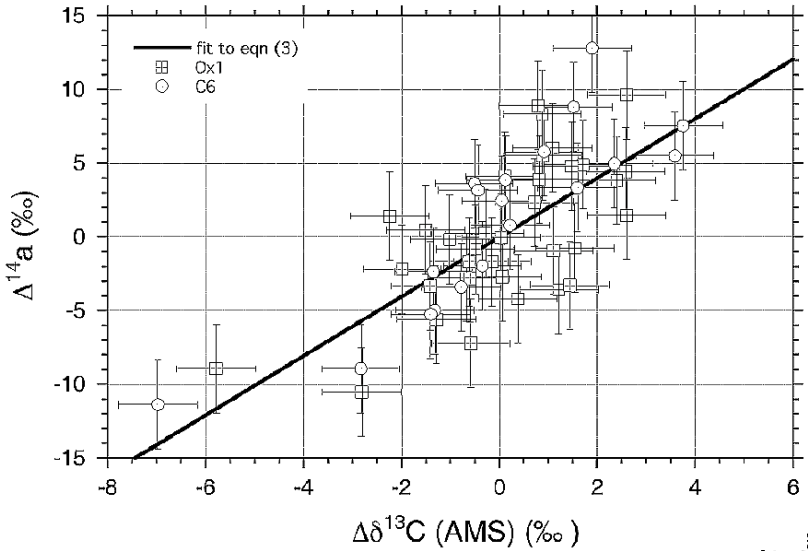

Figure 2 Illustration of the investigation of the $\delta^{13}C_{AMS}$ correction that is routinely applied. Shown is the relation between the difference in $\delta^{13}C_{AMS}$ values for the initial and duplo measurements ($\Delta\delta^{13}C_{AMS}$) and the difference in ^{14}a (Δ^{14}a). The data points are for all Ox1 and C6 measurements in this project. The line is the fit to Equation 3, yielding θ = 1.92 ± 0.23. For further discussion, see text.

The slope is lower than the common value of 2, but not significantly. Theoretically, one would expect θ to be somewhat lower than 2 for most natural fractionation processes (see Mook and van der Plicht 1999), and the ^{13}C-^{14}C relation is likely no exception to this rule. The present finding supports this view to some extent. If one would change the value of θ from 2 to, for example, 1.9, the value of C6 would become ~1.5‰ higher with respect to Ox1, and the atmospheric $^{14}CO_2$ measurements would increase by that amount as well. Of course, before introducing such a major change, more evidence than presented here is needed.

[3]To be exact, the standard deviation after correction will be $\sqrt{1-(0.74)^2}$, 0.67 times the previous standard deviation.

https://doi.org/10.1017/S0033822200038807 Published online by Cambridge University Press

Finally, we checked if the scatter of our $^{14}a_N$ values is indeed lowered by ~33% using $\delta^{13}C_{AMS}$ for fractionation correction using Equation 1. We could check this for the following cases:

- The standard deviation for the scatter of the 8 Ox1 measurements per batch without and with $\delta^{13}C_{AMS}$ correction (^{14}a and $^{14}a_N$) is on average 4.0 and 3.1‰, respectively. Similarly, for IAEA C6 the values are 7.9 and 5.2‰.
- The differences between the initial batches and their measurement duplos are considerably lower, and show considerably less scatter, for $^{14}a_N$ than for ^{14}a. The standard deviation for the ^{14}a difference between the initial batches and measurement duplos is $\Delta^{14}a$ = 6.5‰, whereas for $\Delta^{14}a_N$ this has been lowered to 5.2‰.

The reduction of the standard deviation in the cases above thus fits reasonably well with our expectations.

The conclusion of this detailed look into the $\delta^{13}C$ related matters is a fortunate one; the major part of the $\delta^{13}C_{AMS}$ scatter can be effectively corrected using Equation 1, and thus the spread of the $\delta^{13}C_{AMS}$ values has no significant contribution to the final error in $^{14}a_N$. On the contrary, using the individual $\delta^{13}C_{AMS}$ measurements for fractionation correction (instead of e.g. the IRMS value) improves the final data quality significantly, as illustrated in Figure 2.

The combination of the initial measurement and measurement duplo for each batch, both of them with high counting statistics, proved very worthwhile. One of the remarkable effects visible only because of this methodology was the relation between $\delta^{13}C_{AMS}$ and the ^{13}C current ^{13}I throughout the course of the measurement. This relation was clearly visible in the different signals between initial and measurement duplos, the $\Delta\delta^{13}C_{AMS}$ and $\Delta^{13}I$, and also the $\Delta^{14}a$. As concluded above, the relation disappeared for $\Delta^{14}a_N$. Only in one batch, and only in the initial measurement, did we find that the gradual drift in $\delta^{13}C_{AMS}$ values of 4‰ that related well with ^{13}I caused a sudden jump in ^{14}a. As this jump was documented in both the Ox1 and the C6 measurements and in the difference between initial and measurement duplos, we concluded that this effect must have been caused by a sudden change of the machine settings, and corrected the $^{14}a_N$ values accordingly.

Calibration and Quality Checks

Each of the batches contained 8 Ox1 calibration standards as well as 4 IAEA-C6 reference materials. Our normal calibration procedure would have been to scale the $^{14}a_N$ values of the batch such that the average for the 8 Ox1 samples would be equal to 1.0398, according to the definition of the ^{14}C scale.[4] In this case, however, the extra information provided by the C6 analyses is put to fruitful use. Instead of calibrating each batch using the batch-averaged value for Ox1, we calibrated such that only the average value for Ox1 over the whole set of batches is equal to 1.0398, but allowed for variability between the batches. This variability was used so that the combined error-weighted spread of average Ox1 and C6 values over the batches was minimized. Figure 3 illustrates the procedure. The open symbols show the average values (plus the combined uncertainty in the mean) for Ox1 and C6 per batch for the "standard" case, in which we would define the average values for Ox1 to be 1.0398 for each batch individually. Whereas the Ox1 averages are obviously identical for all batches, the C6 results show a spread that is larger than expected based on the error bars. Of course, this is not the most likely situation (in terms of probability); rather, the spread around the average values is shared between the Ox1 and C6 samples, in an error-weighted way. This is illustrated by the full symbols

[4]In fact, this value is equal to $[(1-25‰) / (1-19‰)]^2 / 0.95 = 1.0397947...$ if we define the $\delta^{13}C$ of Ox1 to be = –19‰ (see Mook and van der Plicht 1999: Equation 6 and following).

https://doi.org/10.1017/S0033822200038807 Published online by Cambridge University Press

in Figure 3. The remaining spread of both Ox1 and C6 is now in accordance with expectations based on their error bars. The difference between the standard calibration and the present recalibration is between 1.5 and –1.5‰ for all batches. Of course, this procedure depends crucially on the uncertainty estimates of the individual measurements. We used the combined uncertainty that is calculated for each measurement by our routine data evaluation program. The combined uncertainty is then the quadratic addition of several uncertainties:

1. The statistical Poisson error;
2. The standard deviation of the background measurements in the batch;
3. The uncertainty in the corrected $^{14}a_N$ due to the standard deviation of the $\delta^{13}C$ of the Ox1 samples in the batch, and finally;
4. The standard deviation of the Ox1 samples in the batch.

As a whole, the combined uncertainty calculated in this way is an overestimation, as sources 1 and 3 influence sources 2 and 4. Our experience (e.g. in ring tests, or "self-check" remeasurements) with this combined uncertainty estimate shows that it is indeed an overestimation, but not by much. In the present recalibration exercise, where the specific ratio of combined uncertainties between C6 and Ox1 matters, it serves its goal well. Although we tried the recalibration procedure using other estimates of combined uncertainty, no alternative did really improve the data compared to our default.

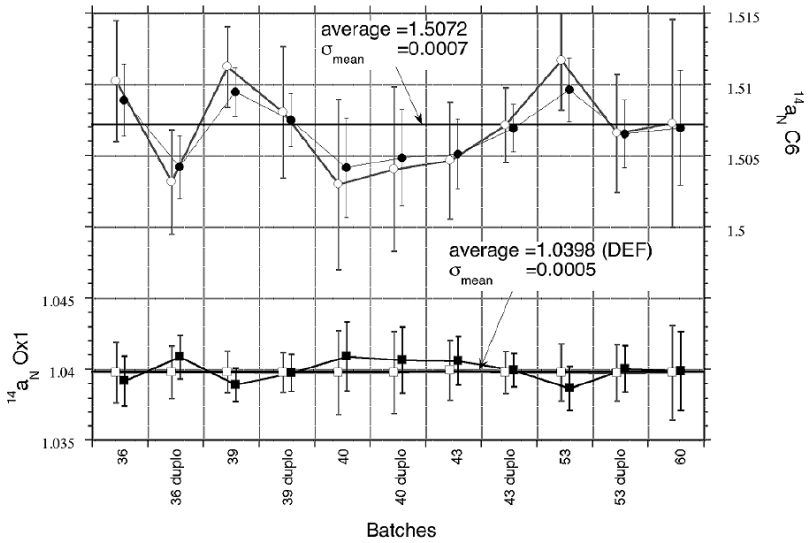

Figure 3 Illustration of the recalibration procedure performed in this work. The *x* axis contains the 11 different batches (5 of which are duplos, that is, a full reanalysis of the same samples), and the 2 *y* axes show the average ^{14}C activity ($^{14}a_N$), with the combined uncertainty in the mean, of the Ox1 samples (left) and the C6 (right). The open symbols show the situation in which calibration has been performed by defining the average Ox1 value per batch to be ≡ 1.0398. The filled symbols show our recalibration result, in which we kept only the total average of Ox1 over all batches to be ≡ 1.0398, but allowed for variability between the batches. This variability was used such that the combined error-weighted spread of average Ox1 and C6 values over the batches was minimized. In this way, the total likelihood of the batch calibration is increased—indicated by the reduced spread of the batch-average C6 results—at the cost of introducing a small spread in the Ox1 values.

To check whether the data indeed benefit from this recalibration procedure, we first compared the differences between the measurement duplos. Figure 4 shows the histograms of the measurement

https://doi.org/10.1017/S0033822200038807 Published online by Cambridge University Press

duplo differences (excluding the Ox1 and C6 samples) of batch 36, both before (a) and after (b) the recalibration. Whereas before the recalibration there existed a significant bias between batch 36 and its duplo of 2.4‰, this bias disappeared after the recalibration. Figure 5 shows the average duplo differences for all 5 batches before (gray bars) and after (black bars) recalibration. All averages are based on 35–40 differences, leading to an error in the mean of slightly below 1‰. The recalibration led to a mostly significantly improved agreement. The right-most column in Figure 5 shows the results for all batches combined. Before recalibration, this value is –1.0 ± 0.4‰ (the error in the mean); after recalibration it shrinks down to –0.3 ± 0.4‰.

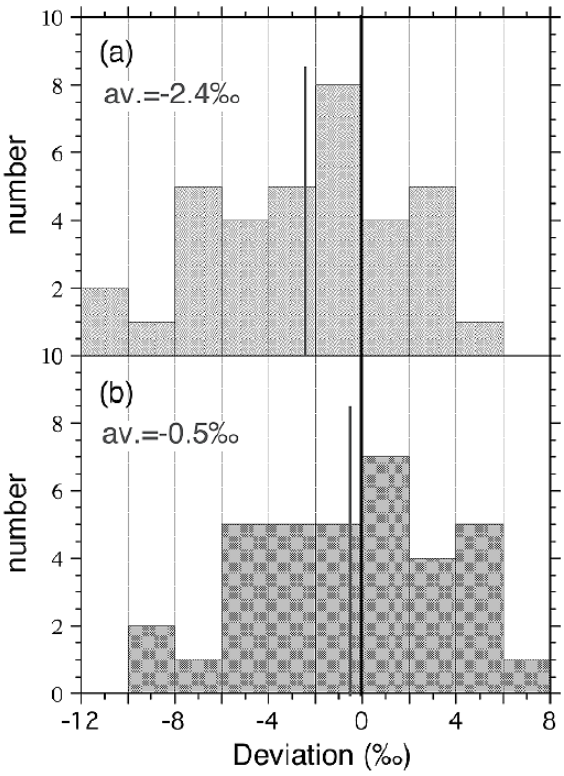

Figure 4 The histograms of the measurement duplo differences (excluding the Ox1 and C6 samples) of batch 36, both before (a) and after (b) the recalibration. See text for further details.

Comparison of the full duplo differences before and after the recalibration provides an even more stringent test. Using this full duplo information, we can compare 5 combinations of batches, along with their measurement duplos, forming a total of 31 (there were an additional 12 full duplos within the batches). Due to the much smaller numbers, however, the results for the average full duplo differences are necessarily less significant. As a whole, the full duplos do not show any bias between the batches, neither before nor after recalibration. The recalibration does, however, decrease the spread of the full duplo differences, and thus improves the total accuracy of the results.

For producing our final results, we obviously use the average values of the initial and measurement duplo measurements. Thanks to the procedures followed, with a complete set of measurement duplos and a considerable number of full duplos, we have ample information for a reliable estimate of

https://doi.org/10.1017/S0033822200038807 Published online by Cambridge University Press

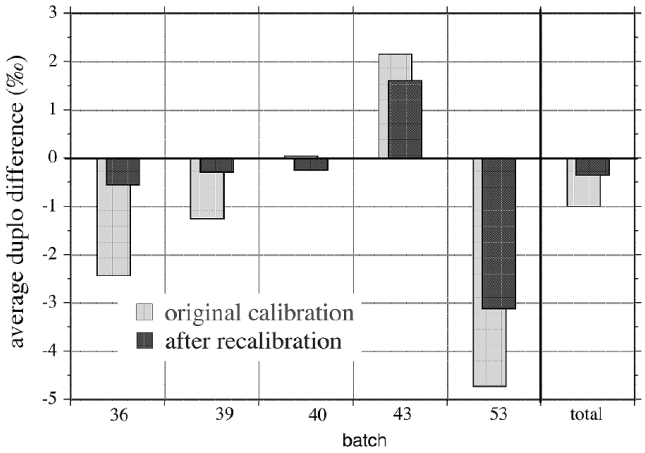

Figure 5 The average duplo differences for all 5 batches before (gray bars) and after (black bars) recalibration. All averages are based on 35–40 differences, leading to an error in the mean of slightly below 1‰. The recalibration led to a mostly significantly improved agreement. The right-most column shows the results for all batches combined. Before recalibration, this value is –1.0 ± 0.4‰ (the error in the mean); after recalibration the value shrinks down to –0.3 ± 0.4‰.

the combined uncertainty of our final measurement results. Table 1 shows the standard deviations that we achieve, both before and after recalibration, and with and without using the average of initial and measurement duplos. Both the measurement duplo procedure and the recalibration worked out positively on the data quality. The improvement (before recalibration) from single to average measurement is not only thanks to the doubling of the number of counts, but also because other errors of a random nature average out. It is thus more rewarding to fully remeasure and independently reanalyze a batch of samples (and average only the final results) than to merely double the measurement time. Also, the recalibration process, or rather the extension of the calibration basis per batch from only Ox1 to Ox1 and C6 combined, appeared to be fruitful. Although it did not remove the largest error source, it improves the data quality significantly because the chance of having systematic biases in the data decreases once more. The effect of the recalibration is illustrated best in the decrease of the C6 standard deviation, at the cost of a slight increase of the standard deviation in Ox1. Based on the numbers in Table 1, our best estimate for the combined uncertainty in a single measurement, for which we take the standard deviation in our data, is ±2.9‰. This number is based on the full duplo differences, as indicated in Table 1. As such, it can be regarded as indeed a reliable number for the combined uncertainty. The calibration uncertainty of ±0.9‰ (based on the standard deviation values for Ox1 and C6 in Table 1, and the number of these samples per batch) and the counting statistics of about ±1.7‰ (an average of 350,000 counts per sample for initial and duplo combined) still make a significant, although not the major, contribution to this number. One might argue that the combined uncertainty claimed here is only the within-laboratory uncertainty and that intercomparison with other laboratories might reveal large(r) discrepancies due to, for example, systematic differences in calibration procedures (including sample preparation). As we will see in the Results section, for global $^{14}CO_2$ work, with its rather small gradients, the combination of data from different laboratories indeed requires intercomparibility at almost the sub-‰ level, and eventual differences at this level are too subtle to be detected in the several large ^{14}C intercomparison exercises that have been performed (Boaretto et al. 2002). These issues need to be addressed separately

https://doi.org/10.1017/S0033822200038807 Published online by Cambridge University Press

through small-scale intercomparison exercises. One such exercise, among the laboratories of Kraków, Heidelberg, and Groningen, is currently underway.

Table 1 The combined uncertainties, expressed as standard deviations, illustrating the averaging effect of the measurement duplos (odd vs. even rows), and the effect of the recalibration (left vs. right column of σs). The standard deviations have been determined using the average differences between the full duplos for the appropriate situations. The averaging leads to a larger gain in accuracy than the recalibration, but this procedure involves the doubling of the available ^{14}C counts. In fact, the decrease in σ is less than the expected: $\sqrt{2}$ if σ were only caused by Poisson statistics (which is obviously not the case). In spite of the relatively low gain in combined statistics, we think the recalibration process is worthwhile, as it decreases the chances for systematic (calibration) deviations, thereby making our claimed combined uncertainty more reliable.

Sample type	σ, initial	σ, after recalibration
full duplo, single measurement	3.9	3.7
full duplo, average measurement	3.0	2.9
Ox1, single measurement	3.1	3.1
Ox1, average measurement	2.0	2.1
IAEA-C6, single measurement	5.2	4.6
IAEA-C6, average measurement	4.6	4.3

Thanks to the many samples of IAEA-C6 that have been analyzed alongside Ox1 samples, we also obtained a new, accurate determination of the activity of IAEA-C6; its average value amounts to 1.5072 ± 0.0007, slightly higher than the consensus value of 1.5061 ± 0.0011 (Rozanski et al. 1992). More results on C6, and also on Ox2, are shown in Table 3 (discussed below).

RESULTS AND DISCUSSION

Results of the Present Analyses

The results for $^{14}CO_2$ records of atmospheric samples from the South Pole and Point Barrow give the final evidence about the success of our effort. Figure 6 shows the results for both records. The general structure of the curves is in accordance with expectations, as the general behavior of $^{14}CO_2$ in air in this period is well known from other sources (Manning et al. 1990; Levin et al. 1992; Meijer et al. 1994; see also "Trends" Web site, http://cdiac.esd.ornl.gov/trends/trends.htm). Also shown are the fits to the data points, being the superposition of a "loess" trend fit with a response time of almost 2 yr (Cleveland 1979) and a single- (South Pole) or double- (Point Barrow) harmonic fit with their amplitude and phase as fit parameters. The upper part of the plots (scale to the right) in Figure 6 shows the residuals from the fits. The standard deviation of these residuals is 3.5‰. This number is larger than the combined uncertainty due to the measurement itself (2.9‰, see Table 1), but obviously this 3.5‰ includes natural variability as well. Thus, we conclude that our goals of performing accurate AMS measurements have been achieved. However, if one would compute the natural variability in the signal by subtracting quadratically the measurement uncertainty of 2.9‰ from the total standard deviation of 3.5‰, one would get to 2.0‰. Although this computation is perhaps naïve, it points out that an even lower measurement uncertainty would still significantly improve the quality of the records. It is also remarkable and fortunate that the grab-sample nature of the present records does not introduce additional natural random variability. Apparently, the sites are remote enough, the ^{14}C signal well-mixed enough, and, of course, the occurring isotope fractionation effects are corrected out of the signal. This encourages the use of flask sampling networks for $^{14}CO_2$ analysis.

https://doi.org/10.1017/S0033822200038807 Published online by Cambridge University Press

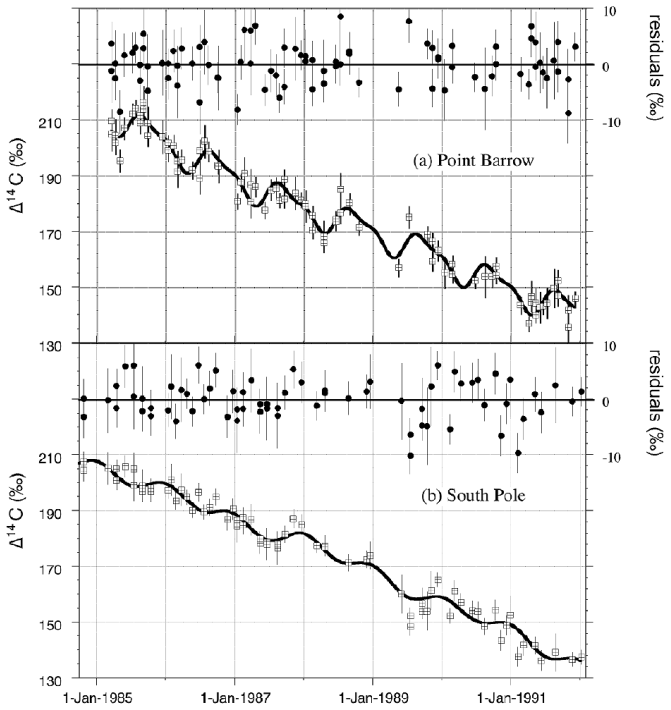

Figure 6 $\Delta^{14}C$ signal for Point Barrow (a) and South Pole (b). See text for details.

Figure 7 shows the data, detrended and brought together irrespective of the specific year, along with the harmonic fit. This representation illustrates the significance of the harmonic fit, even in the case of the South Pole record, more visibly than does Figure 6.

Comparison to Other Records

The present $^{14}CO_2$ records contribute to the global set of $^{14}CO_2$ data that exists thanks to the (in part ongoing) work of several research groups (Nydal and Lövseth 1983; Levin et al. 1992; Manning et al. 1990; Meijer et al. 1994). The 2 records presented here form the northernmost and the southernmost extension to this global data set. Table 2 lists the main characteristics of our new and other available $^{14}CO_2$ records from the same time interval. All of the other stations active at that time produced monthly (sometimes biweekly) mean data from atmospheric CO_2 absorbed in NaOH, measured with proportional gas counters.

During the period of our records, the atmospheric $^{14}CO_2$ level was still elevated due to the nuclear bomb tests of the 1960s, but the stratosphere no longer carried a surplus of $^{14}CO_2$. Ongoing exchange with the ocean still led to a continuous exponential decrease of the atmospheric $^{14}CO_2$ concentration. All records under consideration in Table 2 show this phenomenon. For the interval 1985–1991, this exponential decay is, to a good approximation, linear, and the average slopes of the curves are all near –10‰/yr. Alternatively, exponential fits to the data points yield decay times of between 16.6 and 17.0 yr, in good agreement with the general picture from longer records.

Even more interesting is the detailed comparison of the available records. To this end, we collected the $^{14}CO_2$ data from the electronic and paper sources available and performed the same fit procedures to these records as we did with our own data.

https://doi.org/10.1017/S0033822200038807 Published online by Cambridge University Press

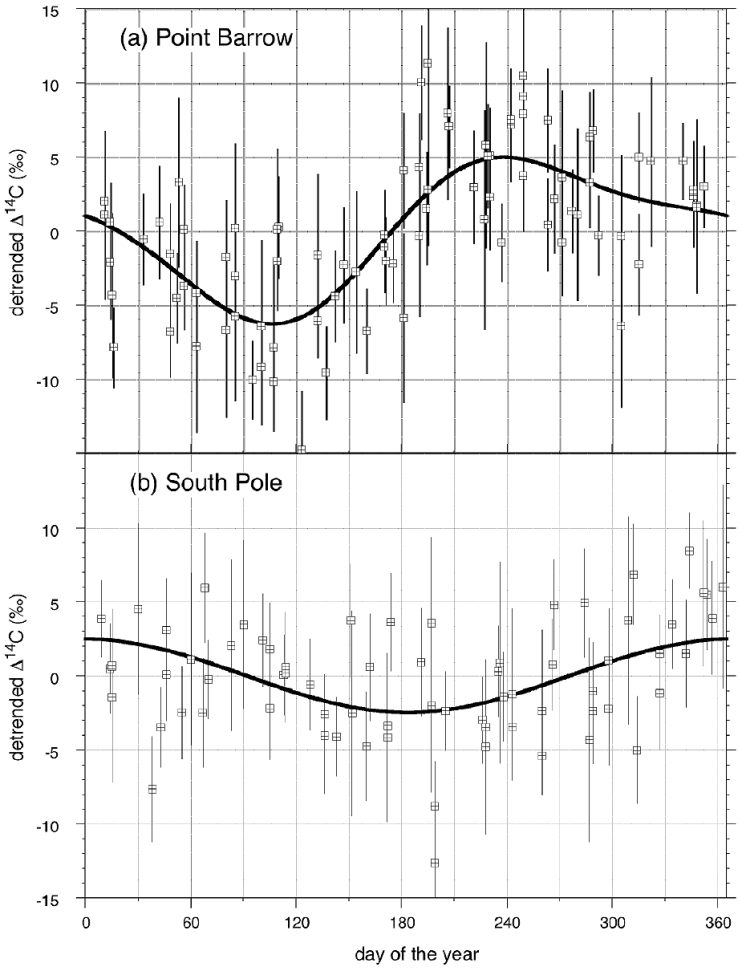

Figure 7 The detrended $\Delta^{14}C$ data for Point Barrow (a) and South Pole (b), brought together irrespective of the specific year, along with the harmonic fits. The Point Barrow fit consists of 2 harmonic functions, with periods of 1 yr and half a year, respectively; South Pole is fitted with only one 1-yr period harmonic. The phases and amplitudes of the harmonics serve as fit parameters (see Table 2).

Figure 8a shows the average levels for the stations considered during 1987 and 1989. This figure is an extension of a similar figure for the same period presented by Levin at al. (1992). The error bars shown are our estimate for the combined uncertainty (±1.5‰), including both the variability of the record and calibration uncertainty. Our Point Barrow data point agrees well with the existing Fruholmen information, but the Fruholmen site might have been slightly affected by European fossil fuel (compare Randerson et al. 2002). Three of the stations are high-altitude (shown in gray and connected with the dashed line) and thus basically probe the free troposphere. The Jungfraujoch and South Pole data agree well with each other for both years; Izaña was higher than those 2 in 1987, but not in 1989. With the South Pole information now available, the influence of the ^{14}C-depleted Southern Ocean south of 60°S (Levin et al. 1992; Levin and Hesshaimer 2000; Randerson et al. 2002) is beautifully demonstrated by the Neumayer-South Pole difference.

https://doi.org/10.1017/S0033822200038807 Published online by Cambridge University Press

Table 2 Comparison of the main features of the Point Barrow and South Pole records with those of other stations that were active in the same 1985–1991 period (Izaña until mid-1990, Neumayer digitized plot data available until 1990, Jungfraujoch started mid-1986, Wellington data used until 1991). Data are given as $\Delta^{14}C$. All data sets have been reprocessed following the identical fit procedures used for Point Barrow and South Pole. The combined uncertainty in the average 1987 and 1989 levels is likely to be mostly dependent on the calibration accuracy of the laboratories involved (our estimate of ±1.5‰ is shown as error bars in Figure 8a). The seasonal cycle has been fitted with either a single 1-yr harmonic with free phase and amplitude, or with 2 harmonics (1 yr and half a year) if the fit improved significantly. This only occurred for Point Barrow and (with less significance) for Fruholmen.

Station	Coord.	Alt. (m asl)	Average 1987 level (‰)	Average 1989 level (‰)	Seasonal peak-through (‰)	Seasonal maximum date	Seasonal minimum date	Ref.[a]
Point Barrow PTB	71.3°N, 156.5°W	11	183.6	165.3	12.0 ± 1.5	Aug 23 ± 7 d	Apr 17 ± 5 d	this work
Fruholmen FRU	71.1°N, 24.0°E	70	182.1	160.9	12.5 ± 2.2	Aug 21 ± 12 d	Mar 27 ± 12 d	b
Jungfraujoch JFJ	46.5°N, 7.7°E	3450	181.2	162.5	6.4 ± 0.6	Sep 7 ± 6 d	Mar 8 ± 6 d	c
Izaña IZN	28.4°N, 16.1°W	2376	185.0	162.7	6.6 ± 1.6	Jul 4 ± 14 d	Jan 3 ± 14 d	b
Wellington WEL	41.3°S, 174.8°E	"low"	181.9	165.0	not significant			d
Neumayer NEU	70.6°S, 8.3°W	16	175.4	155.5	1.8 ± 1.1	Apr 8 ± 35 d	Oct 8 ± 35 d	a, e
South Pole SPO	90.0°S	2810	181.9	161.5	5.0 ± 1.2	Jan 1 ± 13 d	Jul 2 ± 13 d	this work

[a]References: a) Levin et al. 1992; b) Meijer et al. 1994; c) Levin and Kromer 2004; d) Manning et al. 1990 + *Trends*; e) Levin, personal communication.

This powerful influence on the atmospheric $^{14}CO_2$ content through CO_2 exchange with the Southern Ocean is also visible in the seasonal cycle of the Neumayer station, as is shown in Figure 8b. The seasonal patterns in this figure are shown relative to the mean 1987 level of the South Pole. Neumayer shows the Southern Hemisphere phase, "dictated" by the periodicity of stratospheric input, known from the older parts of the Wellington data set (Manning et al. 1990) but shifted towards later in the year by about 2 months. This effect, together with its small amplitude, is a direct measure, both in magnitude and periodicity, for the exchange with the Southern Ocean.

Point Barrow and Fruholmen agree very well, both in their amplitude and in their phase, which is typical for stratospheric input into the Northern Hemisphere (see e.g. the earlier part of the Fruholmen curve in Meijer at al. [1994]). According to Randerson et al. (2002), about half the amplitude of the Fruholmen seasonal cycle is caused by fossil fuel in this period, while for Point Barrow the oceanic influence is more important.

The 3 high-altitude stations all show about the same (smaller) seasonal amplitude (see Table 2). The phase of Jungfraujoch matches those of Fruholmen and Point Barrow, but that of Izaña peaks considerably earlier, resembling the tropical latitude of the site. The phase of the South Pole is surprising, showing its maximum around January 1st. To our knowledge, such a phase (or the opposite in the high Northern latitudes) has not been observed before. This phase puts a new and stringent constraint on model efforts like the one from Randerson et al. (2002).

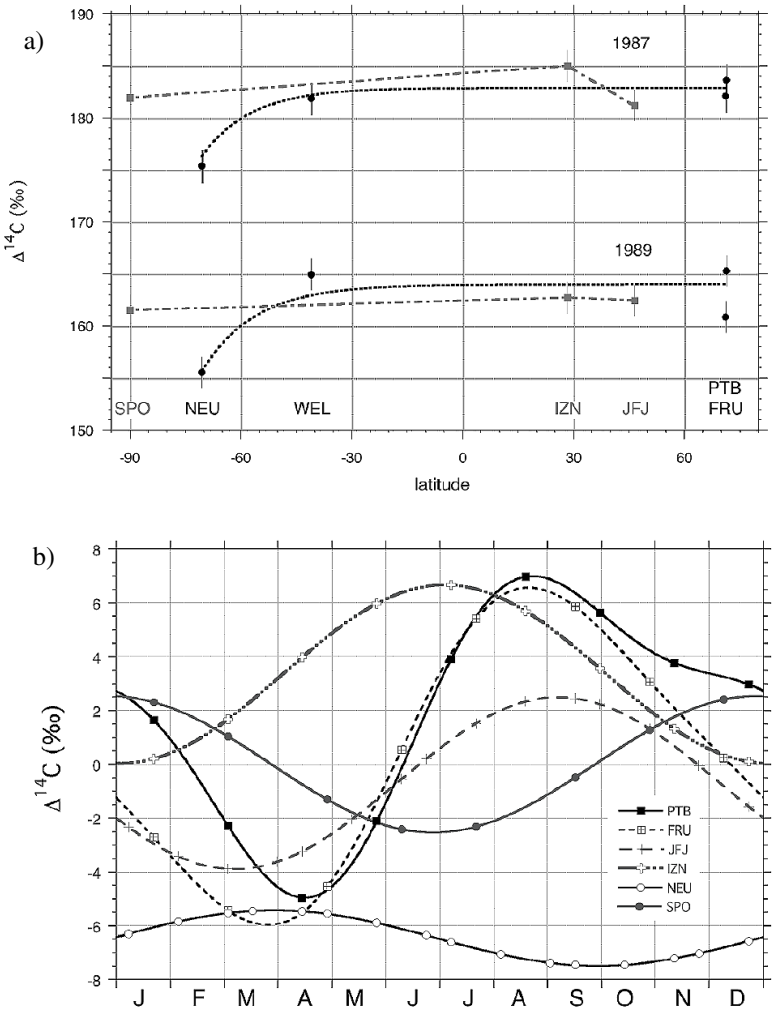

Figure 8 Comparison between the 2 stations presented in this work and a number of stations that were in operation during the same time interval (see Table 2). a) The average 1987 and 1989 levels. The 3 high-altitude stations are shown in gray and connected with the dashed line. The most remarkable feature is the difference between our new South Pole record and that of the Neumayer station (Levin et al. 1992) caused by the influence on the latter by the $^{14}CO_2$-depleted Southern Ocean south of 60°S. b) The fitted seasonal patterns, shown relative to the mean 1987 level of the South Pole. The markers in the lines are for identification purposes only. The differences and similarities in amplitudes and phases are discussed in the text.

Regarding the information presented in Table 2 and Figure 8, we can conclude that both stations, but especially the South Pole, will contribute new and valuable information to the existing $^{14}CO_2$ data set. This extra information can be fruitfully put to use in global modeling efforts, such as those by Levin and Hesshaimer (2000) and Randerson et al. (2002), for carbon cycle research. In particular, the South Pole-Neumayer difference will put a stringent extra constraint on the Southern Hemisphere oceanic exchange. Therefore, it is very unfortunate that the collection of CO_2 from these 2 stations for $^{14}CO_2$ analysis could not be continued for the time after 1991. After a few years, however, ^{14}C-directed sampling and analysis for these 2 stations has recommenced (Heather Graven, personal communication).

https://doi.org/10.1017/S0033822200038807 Published online by Cambridge University Press

CONCLUSIONS AND OUTLOOK

We have demonstrated that by using AMS it is possible to make high-quality measurements with a combined uncertainty of ≤3‰. We also illustrated that this task is by no means trivial. Our procedure of measurement duplos, i.e. analyzing samples twice in 2 fully independent measurement batches, appeared to be fruitful; AMS drifts and variability become more recognizable and are averaged out. Furthermore, our exercise yielded additional data on matters such as fractionation correction.

One obvious further improvement would be to increase the counting statistics. As the Poisson error (~1.7‰ in our case) still contributes significantly, collecting more ^{14}C counts would be a straightforward way to decrease the final combined uncertainty. However, if this has to be achieved by merely analyzing for a longer period, the effect of improved statistics could be impaired by more system variability; increasing the yield of the AMS would be the best way. In our case, we have realized some 30% improvement since the time of these measurements, and a further increase by about the same amount is still feasible. Other AMS installations have even better perspectives in this regard (Turnbull et al. 2006; H Graven, J C Turnbull, personal communication, 2005). A further improvement is position-dependent $\delta^{13}C$ correction. We sputter our targets on 8 different positions, and usually there is some position-dependent $\delta^{13}C$ pattern visible. In the data analysis used thus far (also for the measurements presented here), we used the average $\delta^{13}C$ value for the whole target to perform the $\delta^{13}C$ correction for the total ^{14}C signal. In our newest approach, implemented after—and in part thanks to—the analyses for this paper, we treat a target as the sum of 8 different sub-targets, each with its own $\delta^{13}C$ value. Only the corrected $^{14}a_N$ are finally averaged. Although for good-quality targets, the differences between our former and new methods are minimal; this new correction is yet another step towards the highest possible accuracy. Moreover, it is principally more correct, and might reveal even more insight into the $\delta^{13}C$-^{14}a relation than could be extracted from the present data.

Following the general practice of atmospheric trace gas measurements, it would be logical to monitor the sample preparation route by co-analyzing $^{14}CO_2$ from cylinder air (the local reference). Such a whole-air reference gives direct insight into reproducibility and would directly show contamination, if present. Still, we deem such a local reference not too important, since sample preparation variability mostly only results in isotope fractionation, which is corrected for anyway.

In the quest to achieve a lower combined uncertainty (≤3‰), there are also obstacles of a more principal character. At present, the relative ^{14}C scale is defined using just 1 calibration material (Ox1, but in practice Ox2 for many years). Experience in the stable isotope field (Coplen et al. 2006; Gonfiantini 1984), however, has taught that the interlaboratory consistency benefits very much from the definition of (at least) 1 other calibration material. Although from a principle point of view this is unnecessary and even unwanted (it implies in fact a redefinition of the ‰ on the ^{14}C scale), the practical advantages outweigh the disadvantages. The additional benefit from the definition of such a span calibration is that also the AMS ^{13}C scale would from then on be spanned by 2 calibration points. The handling of the (AMS) ^{13}C signal in general deserves more attention, as does the more principal question of whether or not the ^{13}C normalization towards –25‰ (vs. VPDB) is in fact appropriate for atmospheric CO_2.

Such a span calibration seems at first sight less important for the more classical applications of ^{14}C (such as archaeology). One could, however, limit this new scale agreement to atmospheric $^{14}CO_2$ measurements only, since here the highest accuracy demands apply. It would be an interesting effort to reevaluate the large intercomparisons of the recent past (Boaretto et al. 2002; Scott 2003) by "test-defining" a span calibration and specifically consider the interlaboratory agreement. Of course, such a principal matter requires international agreement, for which the IAEA consultants' group on ^{14}C reference materials (Rozanski et al. 1992) is the most appropriate forum. In this paper, we used the

present 1-point scale definition. In addition to this, however, we present the values that we have found for the IAEA C6 reference material, which would be our potential "span candidate." Table 3 shows our best results for IAEA C6 compared to the consensus values, as well as the average result of measurements for many years from our proportional counters. As we were in the fortunate position that we had a large enough batch of the original Ox1 still available to serve as calibration material for this and other exercises, we can also present our long-term results for Ox2 (that we co-measure with Ox1 and C6), which is the calibration material that officially replaced Ox1. Clearly, the differences between the results are partially significant and indicate once more the usefulness of a span scale. When the consensus values for Ox2 and C6 were established, they had been measured exclusively by proportional counters, and it might be that these installations have a small systematic bias (caused by e.g. sample-to-sample memory in the counters or increased dead time for these "super active" materials) compared to AMS.

Table 3 Our best results for IAEA C6 from the work in this paper compared to the consensus values, as well as to the average result over many years from our proportional counters. Also, our long-term results for Ox2 (that we have co-measured for some time with Ox1 and C6) are shown. See text for details.

Material	$\delta^{13}C$ (vs. VPDB)	$^{14}a_N$ AMS	$^{14}a_N$ PGC	$^{14}a_N$ consensus
Ox1	–19‰ (DEF)[a]	—	—	1.0398 (DEF)[a]
Ox2	–17.6‰[a]	1.3427 (11)	1.3410 (8)	1.3406 (11)[a]
IAEA C6	–10.45‰[b]	1.5072 (7)	1.5035 (5)	1.5061 (11)[c]

[a]Mook and van der Plicht 1999 and references therein.
[b]Coplen et al. 2006.
[c]Rozanski et al. 1992.

We have demonstrated that the AMS technique is now mature enough to also serve those fields with high-accuracy demands, most notably atmospheric CO_2. This clears the way for more records of atmospheric $^{14}CO_2$ from ongoing flask sampling networks, without the burden of installing special (NaOH) sample collection instruments on site, as has been necessary thus far. The first reports on these types of measurements have emerged (Kitagawa et al. 2004; Turnbull et al. 2006) and no doubt will be followed by many more. The data will be made available through the "Trends" program of the Carbon Dioxide Information Analysis Center (CDIAC) (cdiac.ornl.gov/trends/trends.htm).

ACKNOWLEDGMENTS

This work is a spin-off of the long-term cooperation (1976–1992) between the CIO and the Carbon Dioxide Research Group of the Scripps Institute of Oceanography (La Jolla), led by the late C D Keeling. We owe him and his coworkers over the years—for this project in particular, Mrs Alane Bollenbacher—our gratitude for the great cooperation during this time and after. We acknowledge the former chairman of the CIO, W G Mook, for this cooperation as well. The technical staff of the CIO involved in this project, H G Jansen, A Th Aerts, D van Zonneveld, F Gehbru, T F Dijkstra, S Wijma, and H A Been, are thanked for their skillful operation and their extra care for this project.

REFERENCES

Aerts-Bijma ATh, Meijer HAJ, van der Plicht J. 1997. AMS sample handling in Groningen. *Nuclear Instruments and Methods in Physics Research B* 123:221–5.

Boaretto E, Bryant C, Carmi I, Cook G, Gulliksen S, Harkness D, Heinemeier J, McClure J, McGee E, Naysmith P, Possnert G, Scott M, van der Plicht H, Van Strydonck M. 2002. Summary findings of the Fourth International Radiocarbon Intercomparison (FIRI) (1998–2001). *Journal of Quaternary Science* 17(7):633–7.

Cleveland WS. 1979. Robust locally weighted regression and smoothing scatterplots. *Journal of the American Statistical Association* 74:829–36.

Coplen TB, Brand WA, Gehre M, Gröning M, Meijer HAJ, Toman B, Verkouteren RM. 2006. New guide-

lines for $\delta^{13}C$ measurements. *Analytical Chemistry* 78(7):2439–41.

de Jong AFM. 1981. Natural ^{14}C variations [PhD dissertation]. Groningen: Groningen University.

Gonfiantini R. 1984. Advisory group meeting on stable isotope reference samples for geochemical and hydrological investigations. *Report to the Director-General*. Vienna: International Atomic Energy Agency.

International Standards Organization [ISO]. 1993. *Guide to the Expression of Uncertainty in Measurement*. Geneva: ISO. 32 p.

Keeling CD, Whorf TP. 2005. Atmospheric CO_2 concentrations (ppmv) derived from flask air samples collected at Point Barrow, Alaska [WWW document]. URL: cdiac.ornl.gov/trends/sio-keel.htm.

Keeling CD, Bacastow RB, Carter AF, Piper SC, Whorf TP, Heimann M, Mook WG, Roeloffzen H. 1989. A three-dimensional model of atmospheric CO_2 transport based on observed winds: 1. Analysis of observational data. In: Peterson DH, editor. *Aspects of Climate Variability in the Pacific and the Western Americas.* Geophysical Monograph 55. Washington, D.C.: American Geophysical Union. p 165–235.

Kitagawa H, Mukai H, Nojiri Y, Shibata Y, Kobayashi T, Nojiri T. 2004. Seasonal and secular variations of atmospheric $^{14}CO_2$ over the western Pacific since 1994. *Radiocarbon* 46(2):901–10.

Levin I, Hesshaimer V. 2000. Radiocarbon—a unique tracer of global carbon cycle dynamics. *Radiocarbon* 42(1):69–80.

Levin I, Kromer B. 2004. The tropospheric $^{14}CO_2$ level in mid-latitudes of the Northern Hemisphere (1959–2003). *Radiocarbon* 46(3):1261–72.

Levin I, Bösinger R, Bonani G, Francey RJ, Kromer B, Münnich KO, Suter M, Trivett BA, Wölfli W. 1992. Radiocarbon in atmospheric carbon dioxide and methane: global distribution and trends. In: Taylor RE, Long A, Kra RS, editors. *Radiocarbon After Four Decades*. New York: Springer-Verlag. p 503–18.

Levin I, Kromer B, Schmidt M, Sartorius H. 2003. A novel approach for independent budgeting of fossil fuel CO_2 over Europe by $^{14}CO_2$ observations. *Geophysical Research Letters* 30(23): doi: 10.1029/2003GL018477.

Manning M, Lowe DC, Melhuish WH, Sparks RJ, Wallace G, Brenninkmeijer CAM, McGill RC. 1990. The use of radiocarbon measurements in atmospheric studies. *Radiocarbon* 32(1):37–58.

Meijer HAJ, van der Plicht J, Gislefoss JS, Nydal R. 1995. Comparing long-term atmospheric ^{14}C and ^{3}H records near Groningen, the Netherlands with Fruholmen, Norway and Izaña, Canary Islands ^{14}C stations. *Radiocarbon* 37(1):39–50.

Mook WG, van der Plicht J. 1999. Reporting ^{14}C activities and concentrations. *Radiocarbon* 41(3):227–39.

Nydal R, Lövseth K. 1983. Tracing bomb ^{14}C in the atmosphere 1962–1980. *Journal of Geophysical Research* 88(C6):3621–42.

Randerson JT, Enting LG, Schuur EAG, Caldeira K, Fung IY. 2002. Seasonal and latitudinal variability of troposphere $\Delta^{14}CO_2$: post-bomb contributions from fossil fuels, oceans, the stratosphere, and the terrestrial biosphere. *Global Biogeochemical Cycles* 16(4): doi: 10.1029/2002GB001876.

Reimer PJ, Baillie MGL, Bard E, Bayliss A, Beck JW, Bertrand CJH, Blackwell PG, Buck CE, Burr GS, Cutler KB, Damon PE, Edwards RL, Fairbanks RG, Friedrich M, Guilderson TP, Hogg AG, Hughen KA, Kromer B, McCormac G, Manning S, Bronk Ramsey C, Reimer RW, Remmele S, Southon JR, Stuiver M, Talamo S, Taylor FW, van der Plicht J, Weyhenmeyer CE. 2004. IntCal04, terrestrial radiocarbon age calibration, 0–26 cal kyr BP. *Radiocarbon* 46(3):1029–58.

Roeloffzen JC, Mook WG, Keeling CD. 1991. Trends and variations in stable carbon isotopes of atmospheric carbon dioxide. *Stable Isotopes in Plant Nutrition, Soil Fertility and Environmental Studies.* Vienna: International Atomic Energy Agency. p 601–17.

Rozanski K, Stichler W, Gonfiantini R, Scott EM, Beukens RP, Kromer B, van der Plicht J. 1992. The IAEA ^{14}C intercomparison exercise. *Radiocarbon* 34(3): 506–19.

Scott EM. 2003. The Third International Radiocarbon Intercomparison (TIRI) and the Fourth International Radiocarbon Intercomparison (FIRI), 1990–2002: results, analyses, and conclusions. *Radiocarbon* 45(2): 135–408.

Stuiver M, Polach HA. 1977. Discussion: reporting of ^{14}C data. *Radiocarbon* 19(3):355–63

Suess HE. 1955. Radiocarbon concentration in modern wood. *Science* 122:415–7.

Tans PP, de Jong AFM, Mook WG. 1979. Natural atmospheric ^{14}C variation and the Suess effect. *Nature* 280: 826–8.

Trends: A Compendium of Data on Global Change. Carbon Dioxide Information Analysis Center, Oak Ridge National Laboratory, U.S. Department of Energy, Oak Ridge, Tennessee, USA. http://cdiac.ornl.gov/trends/trends.htm. Various contributors.

Turnbull JC, Miller JB, Lehman SJ, Tans PP, Sparks RJ, Southon J. 2006. Comparison of $^{14}CO_2$, CO, and SF_6 for recently added fossil fuel CO_2 and implications for biological CO_2 exchange. *Geophysical Research Letters* 33: doi:10.1029/2005GL024213.

van der Plicht J, Bruins HJ. 2005. Quality control of Groningen ^{14}C results from Tel Rehov: repeatability and intercomparison of proportional gas counting and AMS. In: Levy TE, Higham T, editors. *Radiocarbon Dating and the Iron Age of the Southern Levant: The Bible and Archaeology Today.* London: Equinox Publishing. p 256–70.

van der Plicht J, Wijma S, Aerts AT, Pertuisot MH, Meijer HAJ. 2000. Status report: the Groningen AMS facility. *Nuclear Instruments and Methods in Physics Research B* 172:58–65.